ELSEVIER

Journal of Photochemistry and Photobiology A: Chemistry 140 (2001) 163–172

Journal of Photochemistry and Photobiology A:Chemistry

www.elsevier.nl/locate/jphotochem

Photooxidative *N*-demethylation of methylene blue in aqueous TiO_2 dispersions under UV irradiation

Tianyong Zhang [a,1], Toshiyuki Oyama [a], Akio Aoshima [a], Hisao Hidaka [a,*], Jincai Zhao [b], Nick Serpone [c]

[a] *Frontier Research Center for the Global Environmental Protection, Meisei University, 2-1-1 Hodokubo, Hino-shi, Tokyo 191-8506, Japan*
[b] *Institute of Chemistry, Chinese Academy of Sciences, Beijing, PR China*
[c] *Department of Chemistry and Biochemistry, Concordia University, 1455 de Maisonneuve Blvd West, Montreal, Canada H3G 1M8*

Received 23 October 2000; received in revised form 4 January 2001; accepted 19 January 2001

Abstract

Methylene blue (MB) is a representative of a class of dyestuffs resistant to biodegradation. Its decomposition was examined in aqueous TiO_2 dispersions under UV illumination to assess the influence of temperature, pH, concentration of dissolved oxygen (DOC), initial concentration of MB, and light intensity on the kinetics of decomposition. Hypsochromic effects (i.e. blue shifts of spectral bands) resulting from *N*-demethylation of the dimethylamino group in MB occurs concomitantly with oxidative degradation. The maximum quantity of MB adsorbed on TiO_2, and the kinetics of degradation of MB and of total organic carbon (TOC) removal were also measured at constant pH 4. Photobleaching of MB solutions takes place at low DOCs and is caused by a reversible reductive process involving photogenerated electrons on TiO_2. The rate of degradation of MB remains fairly constant regardless of whether the dispersion was purged with oxygen prior to irradiation or with air during the light irradiation period. The photocatalytic process depends on light intensity, but not on the total light energy absorbed. The photoreaction followed pseudo-first-order kinetics even at high MB concentrations (0.3 mM). The temperature dependence of the photodegradation kinetics was assessed ($E_a = 8.9$ kJ/mol), as well as the relative photonic efficiency, ξ_r, relative to phenol (0.48).

Keywords: Methylene blue; Photocatalytic reaction; Titanium dioxide; *N*-demethylation

1. Introduction

Textile dyes and other commercial colorants have become the focus of environmental remediation efforts because their natural biodegradability is made increasingly difficult owing to improved properties of dyestuffs [1,2]. Many dyes are highly water-soluble in order to meet the color requirement of deep dyeing. Consequently, traditional wastewater treatment methods such as flocculation, activated carbon adsorption, and biological treatment are increasingly ineffective.

Earlier studies [3–12] showed that electron transfer between dyes and nanosized semiconductor particles occurs under visible and UV irradiation, and that dyes can be degraded to smaller organic substances and ultimately mineralized completely to water, carbon dioxide, and other inorganic ions. Utilizing these processes to degrade colored organic pollutants, such as dyes, has important implications because they can make use of visible light or natural sunlight. The data reported recently in the literature on the photocatalyzed degradation of certain dyes by a heterogeneous photocatalytic process are not sufficient for industrial or for large scale pilot plant applications because several experimental parameters (e.g., light intensity, reactor geometry, pH, temperature, concentration and structure of reactant and concentration of TiO_2) have complex effects on the degradation reaction and thus also on treatment cost [13].

Heterogeneous photocatalysis through illumination of aqueous suspensions of TiO_2 offers an attractive advanced oxidation technology that is capable of purifying waste-waters [14]. The photocatalyzed degradation of methylene blue (MB) has been reported for TiO_2 thin films [15] and in aqueous TiO_2 suspensions using simulated or natural sunlight [16–18]. However, hypsochromic effects, and the dependence of the photodegradation on dissolved oxygen concentration (DOC), temperature, light intensity,

* Corresponding author. Tel.: +81-44-591-6635; fax: +81-44-599-7785.
E-mail address: hidaka@epfc.meisei-u.ac.jp (H. Hidaka).
[1] Permanent address: Department of Applied Chemistry, College of Chemical Engineering and Technology, Tianjin University, Tianjin 300072, PR China.

1010-6030/01/$ – see front matter
PII: S1010-6030(01)00398-7

initial substrate concentration, and changes in total organic carbon have received only scant attention. MB resists photolytic degradation.

Herein, we examine the photodegradation of MB in aqueous TiO_2 dispersions under UV light irradiation. The influence of temperature, pH, DOC, initial concentration of MB, and light intensity on the degradative process was studied in detail. Both hypsochromic effects arising from *N*-demethylation of MB and oxidative degradation occur concomitantly under irradiation. At low DOCs, MB solutions are photobleached, caused by a reversible reductive reaction owing to insufficient available oxygen to scavenge the electrons photogenerated on TiO_2. Photocatalytic decomposition rates of MB showed only slight changes with variations of the total absorbed light energy, but scaled with light intensity. At relatively high concentrations (e.g., 0.3 mM), the photoreaction followed pseudo-first-order kinetics. The relative photonic efficiency (with respect to phenol) and the activation energy of the photodegradative process were determined. Experimental results provide some of the needed information toward application of the heterogeneous photocatalytic method to degrade dyestuffs on a pilot plant scale using solar light collectors as irradiation sources.

2. Experimental

2.1. Materials

The nanosized TiO_2 photocatalyst was supplied by Degussa (P-25, surface area ~50 m^2/g by BET methods; mean diameter ca. 30 nm by TEM microscopy; 87% anatase and 13% rutile determined by X-ray diffraction). MB (as the hydrochloride salt containing three water molecules) was obtained from Kokusan Chemical Works (special grade). For reference, the structures of MB and some of the related derivatives and potential degradation intermediates in the photodegradation are illustrated in Fig. 1.

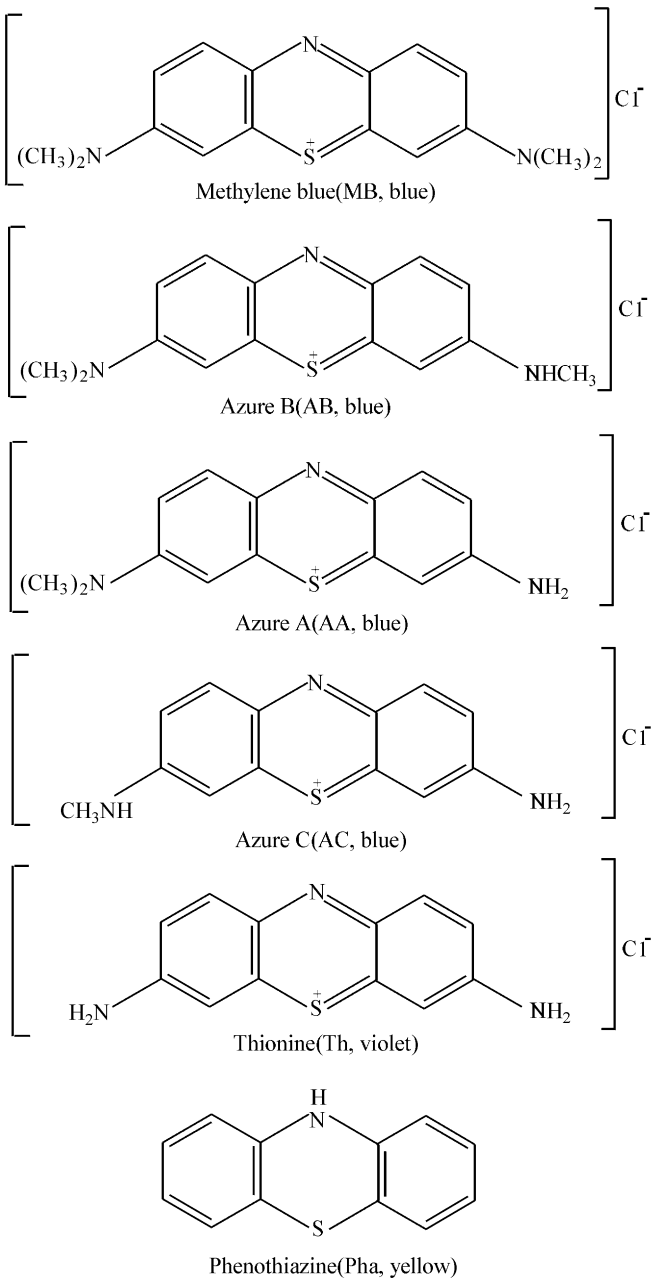

Fig. 1. Chemical structures of MB and of related *N*-demethylated intermediates, and phenothiazine.

2.2. Photodegradation procedures and analytical methods

Ion-exchanged water was used for the reaction solution (50 ml) containing MB (0.1 mM) and 100 mg of TiO_2 particulates in a 124 ml cylindrical Pyrex photoreactor. The initial pHs of the solutions were adjusted by addition of HCl or NaOH solutions prior to addition of TiO_2, as necessitated by the experimental conditions. After the reaction mixtures were dispersed for ca. 5 min in an ultrasonic bath, the aqueous dispersions were saturated with dissolved oxygen (analyzed for DOC with a Horiba DOC meter Model DO 25) by purging the dispersion for about 10 min with molecular oxygen. Overall, UV irradiation of aqueous TiO_2 dispersions was carried out either under an oxygen atmosphere, or air-equilibrated conditions, or under a nitrogen atmosphere employing a 75 W Hg lamp (Toshiba SHL-100 UVQ-2), which delivered the desired photon flux (UV Radiometer, Model UVR-2 UD-36, Topcon) in the wavelength range 310–400 nm (maximum emission at λ_{max} = 360 nm). The photon flux incident on the photoreactor was varied by adjusting the distance between the photoreactor and the mercury lamp. Vigorous magnetic stirring was maintained to keep the TiO_2 particles suspended in the dispersion. A 3 ml aliquot was sampled at various time intervals; it was centrifuged and then filtered through a millipore membrane filter (pore size 0.2 μm) prior to analyses. Variations in the concentration of MB in each degraded solution were monitored by UV–visible spectroscopy (JASCO V-570

spectrophotometer; $\lambda_{max} = 612$ nm). Changes in total organic carbon (TOC) were determined using a Shimadzu total organic carbon analyzer (Model TOC-5000A).

3. Results and discussion

3.1. Photocatalytic decomposition of MB

Temporal changes in the concentration of MB were monitored by examining the variations in maximal absorption in UV–visible spectra at 660 [15,18] or 665 nm [17]. Typically, MB solutions display maximal absorbance at 668 and 609 nm [19]. Under our experimental conditions, maximal absorption occurred at 664 and 612 nm at pHs 1–7 (see e.g. Fig. 2A). The latter absorption band was selected to monitor the temporal concentration changes of MB in aqueous TiO_2 dispersions, since the band at 664 nm shifted considerably towards the blue region during the course of the photoassisted degradation (this aspect will be discussed in some detail later).

Results of the degradation of MB in the presence and absence of TiO_2 under UV irradiation are illustrated in Fig. 2C, which also shows significant temporal concentration changes of MB. In the absence of TiO_2, MB degraded neither under UV irradiation nor in the dark. MB degraded by a TiO_2-assisted photocatalytic oxidative process [20,21] via good first-order kinetics, $k = 3.02 \pm 0.08 \times 10^{-3}\ \text{min}^{-1}$ (Fig. 2C).

Related to the present observations, blue shifts of the absorption bands seen during the photooxidative *N*-deethylation of auxochromic groups in the Rhodamine B substrate in aqueous semiconductor dispersions were reported earlier by us [22,23], and elsewhere by others [24–26]. *N*-demethylation of MB was observed by Mohammad and Morrison [27] during "photodynamic therapy" studies using visible light irradiation ($\lambda > 520$ nm). *N*-dealkylation of dyes containing auxochromic alkylamine groups plays an important role in photocatalytic degradation. The color of MB solutions becomes less intense (hypsochromic effect) when all or part of the auxochromic groups (methyl or methylamine) degrade. Fig. 2A and B also shows that the spectral band at 664 nm blue-shifts by as much as 54 nm from 664 to 610 nm during the course of the photodegradation. We contend that *N*-demethylation of MB occurs as described in the pathway depicted in Fig. 3, where AB, AA, AC and Th refers to the various structures of the *N*-demethylated intermediates of Fig. 1. As weak electron-donor substituents, methyl groups can facilitate attack on MB by electrophilic species ($^{\bullet}OH$ or h^{+}_{vb}) in the demethylation process; this is also likely to be a major step in the photocatalytic oxidative degradation of MB. Examination of the spectral variations in Fig. 2A and B suggests that MB was *N*-demethylated in a stepwise manner (i.e., methyl groups were removed one at a time as confirmed by the gradual peak wavelength shifts toward the blue

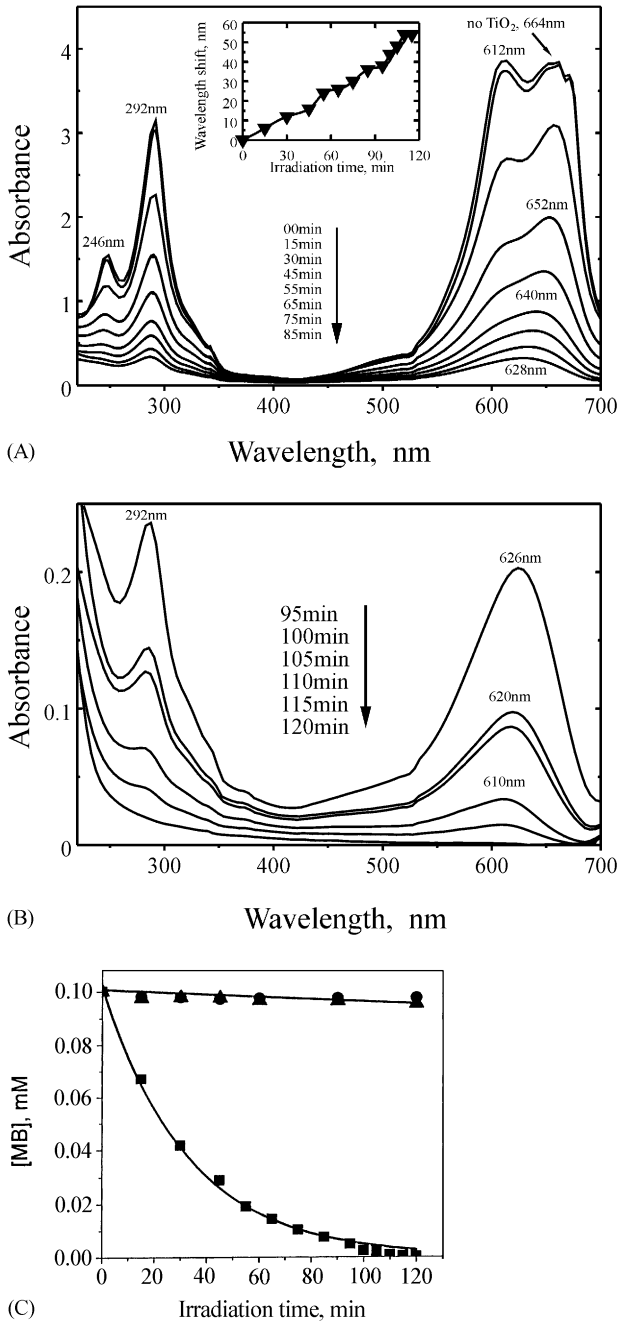

Fig. 2. (A) Temporal spectral changes of MB in aqueous TiO_2 suspensions under UV illumination (0–85 min); experimental conditions are otherwise identical to those of UV-irradiated TiO_2 dispersions in (C). Inset shows the wavelength blue-shifts of the 664 nm band. (B) Continuation of the temporal spectral changes of (A); irradiation times, 95–120 min. (C) Photodegradation of MB in the presence and absence of TiO_2 in 50 ml dispersions under UV irradiation (MB, 0.1 mM; pH 3.85; TiO_2 loading, 100 mg; light irradiance, 5.3 mW/cm^2 at $\lambda = 360$ nm). (■), UV-irradiated TiO_2; (●), direct UV photolysis without TiO_2; (▲), in the dark with TiO_2.

region), with cleavage of the MB chromophore ring structure (phenothiazine or thionine) occurring concomitantly as evidenced by the decrease in TOC (see below).

Absorption bands of *N*-demethylated analogs of MB in the visible range are seen [19] at 648–655 nm for Azure B (blue

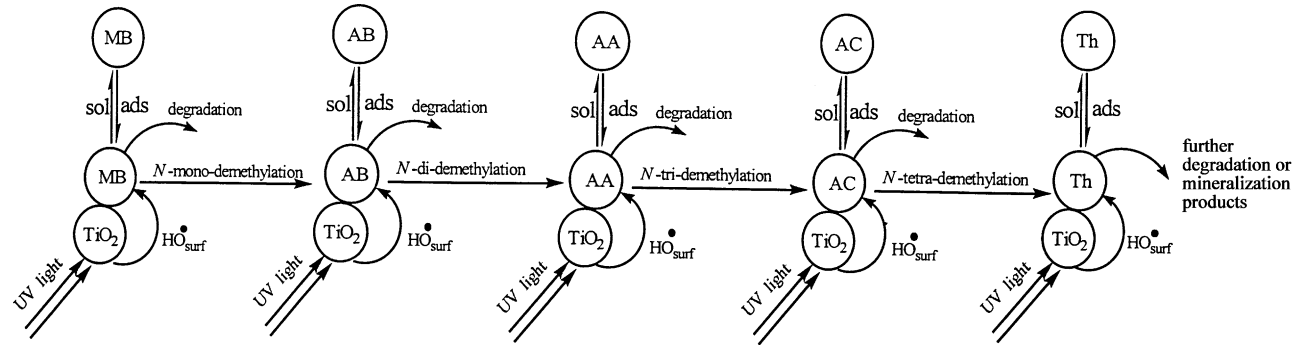

Fig. 3. Scheme depicting the *N*-demethylation of MB and the dynamic equilibrium of MB and *N*-demethylated species between the bulk solution and the TiO_2 particle surface during the photodegradation of MB.

color in aqueous solution), at 620–634 nm for Azure A (blue color in aqueous solution), at 608–612 nm for Azure C (blue color in aqueous solution), and at 602.5 nm for Thionine (first yields a blue color, then a violet solution). These characteristic bands are also discernible in Fig. 2A and B. The color of TiO_2 particles turned from white to a grayish blue color, and then to a grayish pink color caused by mixtures of colored intermediates adsorbed on the surface of the particles and undergoing partial or complete *N*-demethylation and deamination during irradiation. Note that the pink coloration could still be seen after the blue color of the solution had disappeared. Continued UV illumination caused the pink intermediates to also degrade bringing the TiO_2 dispersion back to its original state (white). After 115 min of irradiation, a broad band appeared around 610 nm (Fig. 2B), which likely masked the less intense 602.5 nm band of Thionine since the dispersion was still bluish. Thionine is somewhat insoluble in water and consequently tends to adsorb on the surface of TiO_2. The bands at 292 and 246 nm decreased significantly with irradiation time and no new bands appeared. This implies that full oxidative decomposition of the phenothiazine species had occurred and that other intermediates containing the phenothiazine moiety no longer formed. *N*-demethylation, deamination and oxidative degradation take place during the photocatalyzed degradation of MB. Mixtures of *N*-demethylated intermediates yield spectra with broad absorption bands in the visible range.

3.2. pH dependence of the photocatalytic degradation of MB

Rates of the photocatalytic degradation of MB in aqueous TiO_2 dispersions (Table 1 and Fig. 4A) and the blue shifts of the absorption bands of MB solutions (Fig. 4B) are pH dependent. Wavelength shifts at pH = 1.85 are nearly negligible and the degradation rate was slowest; greater wavelength changes were observed at other pHs, with the greater change occurring at pH = 3.85. It would seem that *N*-demethylation promotes photooxidative degradation of MB.

Maximal adsorption, apparent rate constants and rates of TOC removal were obtained at pH ∼ 4 (Fig. 5). Adsorption

Table 1
pH dependence of the kinetics for the photodegradation of MB in UV-illuminated aqueous TiO_2 dispersions

pH	k (10^{-2} min^{-1})
1.85	0.30 ± 0.10
2.98	1.69 ± 0.08
3.85	3.16 ± 0.07
5.32	1.12 ± 0.05

of MB on the surface of TiO_2 strongly affects the degradative process. The extent of adsorption of MB on TiO_2 is relatively small, about 4% at pH ∼ 4 (Fig. 5A). Consistent with this assertion, although the color of the bulk solution was

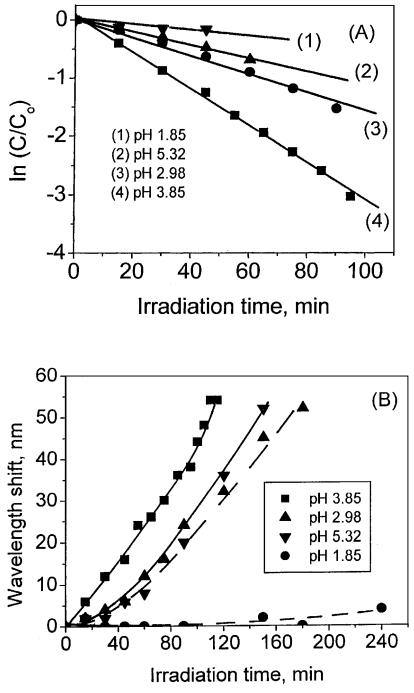

Fig. 4. (A) Reaction rate kinetics vs. pH values in 50 ml aqueous TiO_2 dispersions under UV light illumination (MB, 0.1 mM; TiO_2 loading, 100 mg (P-25); 75 W Hg lamp; light irradiance, 5.3 mW/cm^2 at λ = 360 nm). (B) Effect of pH on the wavelength blue shifts of the 664 nm band of MB in aqueous UV-irradiated TiO_2 dispersions. Experimental parameters are the same as those in (A).

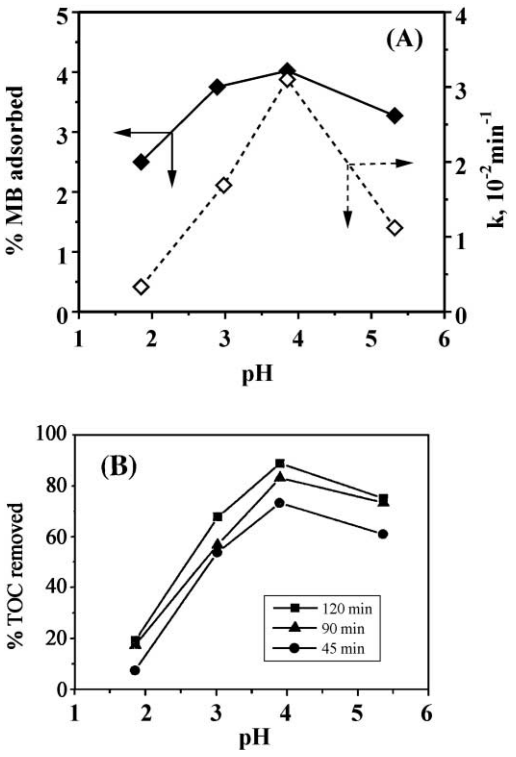

Fig. 5. (A) Extent of adsorbed amount of MB on TiO_2, apparent rate constant and (B) TOC removal of MB in the course of photodegradation at various pHs in 50 ml aqueous UV-illuminated TiO_2 dispersions (MB, 0.1 mM; TiO_2 loading, 100 mg; light irradiance, 5.3 mW/cm^2 at $\lambda = 360$ nm).

initially an intense blue, even when adsorption/desorption equilibrium had been reached, the TiO_2 particles were only slightly light blue colored.

MB adsorbs on TiO_2 through the nitrogen atoms that hydrogen bond to the surface hydroxyl groups. By contrast, the MB cationic dye is strongly repelled by the positively charged TiO_2 particles, particularly, when the pH of the aqueous dispersion is less than the pH_{pzc} of TiO_2 (the point of zero charge, pH_{pzc}, is ca. 6.8 for Degussa P-25 under certain conditions [28]). In our experiments, the pH was constantly lower than the pH_{pzc} of TiO_2, so that the extent of adsorbed MB on TiO_2 tends to be small. Maximum adsorption occurs at pH $\sim$ 4. The maximal photodegradation rate for MB also occurs around pH 4 and decreases at pH ca. 5. We do not preclude a $pH_{pzc} \sim 4$ since the point of zero charge (pzc) depends on the nature of the dispersion.

After ca. 120 min of UV irradiation, the bulk solution of the aqueous TiO_2 dispersions turned completely colorless and was accompanied by approximately 90% TOC removal (Fig. 5B). Some colorless intermediates were still dissolved in the bulk solution, while other light violet-colored intermediates were adsorbed on the TiO_2 surface. On further irradiation, TOC removal increased; TOC removal was enhanced to 98.9% at pH 3.85 after 240 min, albeit the rate of TOC removal was somewhat slower between the two irradiation periods. The increase in TOC removal from pH 1.85 to 3.85 (Fig. 5B) clearly shows that the phenothiazine structure of the MB cations, and the methyl groups removed by the demethylation process were converted to smaller organic species and ultimately mineralized to inorganic products (the fate of N atoms was not examined in this study).

3.3. Effect of DOC on the photoassisted oxidative reaction

The quantity of oxygen actually adsorbed on the surface of TiO_2 particles is difficult to assess; it should scale with the level of DOC in the bulk solution. Also, the DOC level in aqueous TiO_2 dispersions should strongly influence the photocatalyzed degradative process since oxygen suppresses/prevents recombination of photogenerated electrons (e^-_{cb}) and holes (h^+_{vb}).

Hasegawa et al. [29] recently examined how the partial pressure of oxygen affects the kinetics of the photocatalyzed degradation of some agrochemicals in aqueous TiO_2 dispersions. The shortcoming of the partial pressure method is that it does not provide a means to assess the specific role of oxygen in photocatalyzed degradations. For example, the partial pressure of oxygen at the interface between air and river or lake waters hardly changes, yet fish and other aquatic organisms die as a result of insufficient DOC levels in those waters because oxygen may be exhausted by water pollution. In the other extreme case, oxygen partial pressure may be greater than atmospheric pressure, yet DOC levels may still be insufficient for the photocatalytic processes in large scale plant treatments. Consequently, the influence of DOC on photodegradation was worth investigating.

The DOC level in the ion-exchanged water used in our experiments ranged between 6.0 and 8.5 mg/l (experimentally measured). DOC can be increased by purging the aqueous titania dispersions with oxygen gas and decreased by purging with such inert gases as nitrogen or argon. The effects of DOC on the apparent first-order kinetics are displayed in Fig. 6A and B; for removal of TOC they are depicted in Fig. 6C. When DOC was less than $\sim$5 mg/l, both k_{app} and TOC removal were significantly diminished; the latter increased slightly when DOC was greater than 5 mg/l. Clearly, the presence of sufficient oxygen to scavenge the photogenerated electrons is necessary to suppress electron/hole recombination in heterogeneous photocatalytic processes. Our data indicate that 5 mg/l of DOC meets that requirement in the photodegradation of MB. A decrease of DOC in TiO_2 dispersions impacts negatively on the photocatalytic rate.

Another important phenomenon was seen at the lowest DOC levels in the dispersions. When DOC was 0.16 or 0.32 mg/l, the reaction solution turned colorless fairly rapidly after only ca. 10 min of UV irradiation. The blue color of the dispersion was restored when irradiation was stopped and the system exposed to atmospheric oxygen for a short time (ca. 5–10 min). We deduce that the

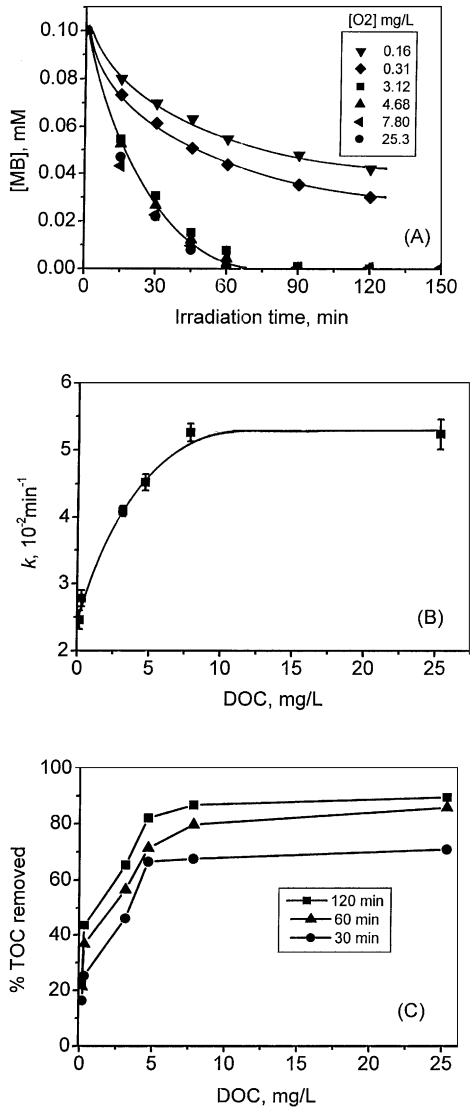

Fig. 6. Effect of the level of DOC in 50 ml aqueous titania dispersions on the photocatalytic decomposition rate and TOC removal of MB under UV light illumination (MB, 0.1 mM; pH 3.85; TiO_2 loading, 100 mg (P-25); light irradiance, 5.3 mW/cm^2 at 360 nm).

dispersion was photobleached and that MB was not oxidized (however, see below); the photobleach process was reversible. Photogenerated electrons reduce MB to produce the colorless leucomethylene blue species (Eq. (1)), which is readily oxidized to the MB precursor by oxygen [30]. When DOC is sufficient to trap the photogenerated electrons, Eq. (1) is

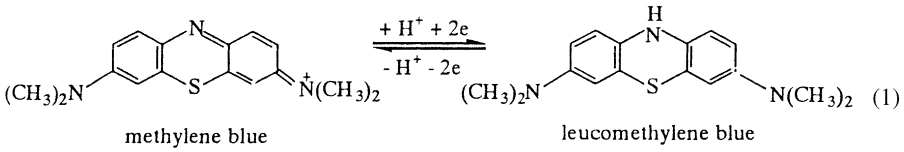

(1)

inconsequential, or at least it is not detectable under our prevailing experimental conditions. UV–visible spectral results indicate that no oxidative demethylation derivatives of MB formed during the formation of leucomethylene blue, despite the small quantity of TOC removed at the low DOC levels (see Fig. 6C). To the extent that not all the dissolved oxygen was removed by nitrogen purging (see e.g. Fig. 6A), this decrease in TOC may have been caused by some oxidation of MB.

3.4. Effect of the mode of providing oxygen to the photocatalytic reaction

We have seen so far that DOC plays an essential role in the photocatalyzed degradation of MB. Fig. 7A illustrates the kinetic results (average $k_{app} = 4.9 \pm 0.2 \times 10^{-2}\,min^{-1}$) of the effect of four methods by which oxygen was supplied to the aqueous TiO_2 dispersions. With Method I, namely purging the dispersion continuously with oxygen during the photocatalytic process, the DOC level increased to about 25.0–40.0 mg/l; with Method II (i.e., without oxygen bubbling) the level of DOC was maintained around 7.8 mg/l (air-equilibrated conditions); with Method III, when the dispersion was purged continuously with air during the photocatalytic process, it was possible to maintain the level of DOC at about 8.0–8.5 mg/l (note that DOC cannot be increased beyond this level by this method); with Method IV, in which the dispersion was purged with oxygen only prior to UV irradiation, the DOC level was as much as 25.0–40.0 mg/l initially, but then DOC decreased rapidly to ca. 8.4 mg/l by vigorous mechanical stirring.

In general, the higher DOC level in the dispersions could be maintained by means of Method I, whereas both Methods III and IV could not provide greater levels of DOC than possible with Method II. Experimental results illustrated in Fig. 7A shows that there is no difference in the degradation rate, whether or not the dispersion is purged with oxygen. Dioxygen dissolves fairly rapidly (k_{O_2}(dissolution) = $4.1 \times 10^{-2}\,min^{-1}$) in aqueous TiO_2 dispersions from the air atmosphere by simple but vigorous mechanical stirring (Fig. 7B) if the ratio of the surface area of the dispersion exposed to air (12.56 cm^2) to the reaction volume (50.0 cm^3) is relatively large (0.25 in the present instance). An experiment with a modified Method IV, in which the photoreactor was closed with a stopper, also showed that the apparent rate of degradation of MB was nearly identical to the rate obtained by Method IV.

When wastewater treatment is conducted in large scale plants, it is not unlikely for the operative conditions to be different from those described here. For example, mechanical stirring efficiency may decline, or the ratio of the

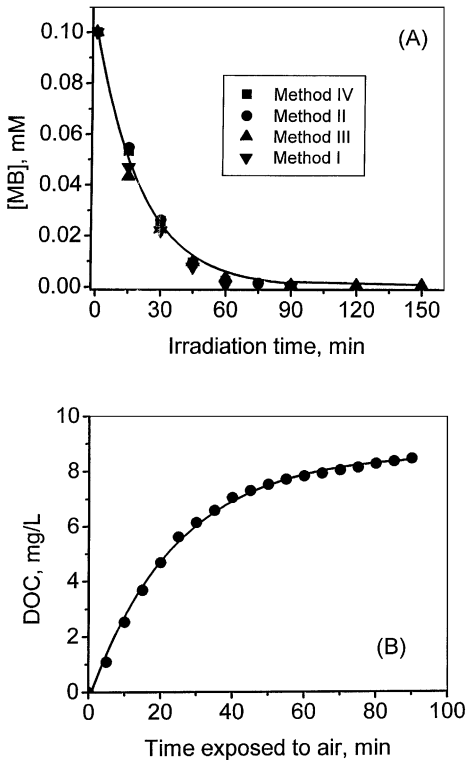

Fig. 7. (A) Comparisons of the kinetics of MB photodegradation under conditions where different methods are used to supply oxygen to the 50 ml aqueous TiO_2 dispersion (MB, 0.1 mM; pH 3.85; TiO_2 loading, 100 mg (P-25); light irradiance, 5.3 mW/cm^2 at 360 nm). Method I, purging the dispersion continuously with dioxygen during UV light irradiation. Method II, exposure of the aqueous TiO_2 dispersion to the atmosphere (air-equilibrated conditions). Method III, purging the dispersion with air continuously during UV light irradiation. Method IV, the aqueous TiO_2 dispersion was saturated with oxygen prior to UV light irradiation in a closed photoreactor — no oxygen or air was supplied during irradiation. (B) Kinetics of dissolution of oxygen from air in a 50 ml aqueous TiO_2 dispersion agitated with a magnetic stirrer (MB, 0.1 mM; pH 3.85; TiO_2 loading, 100 mg (P-25)). The aqueous TiO_2 dispersion is exposed to air.

surface area exposed to the atmosphere to the reaction volume may be smaller, not to mention the obvious variations in photoreactor geometry and size. Most relevant, however, the wastewaters are likely to consist of a complex mixture of tens to hundreds of pollutants, many of which are of unknown origin. Consequently, utilization of a method that forces high levels of DOC in the dispersion may help to promote mass transfer efficiency and maintain the much needed adequate supply of DOC. It must be emphasized that experimental conditions will bear heavily on large scale wastewater treatment operations.

3.5. Effect of the initial concentration of MB on the kinetics of photodegradation

The kinetics of photodegradation of MB in UV-illuminated aqueous TiO_2 dispersions under ambient conditions changes with the initial concentration of MB (Table 2 and Fig. 8A). Fig. 8B illustrates the relationship between the

Table 2
Concentration dependence of the kinetics of photodegradation of MB

C_0 (mM)	R_0 (10^{-3} mM min^{-1})	k_{app} (10^{-2} min^{-1})
0.02	2.0	90.0 ± 13.0
0.04	2.4	9.7 ± 0.4
0.08	3.0	5.5 ± 0.2
0.10	3.0	4.6 ± 0.3
0.15	4.0	3.0 ± 0.3
0.30	4.8	1.5 ± 0.1

initial concentrations, C_0, and the initial reaction rates, R_0, a relationship that parallels the expectations of the Langmuir–Hinshelwood model (Eq. (2)):

$$\frac{1}{R_0} = \frac{1}{k} + \frac{1}{kKC_0} \quad (2)$$

where k is the apparent zero-order rate constant ($5.05 \pm 0.06 \times 10^{-3}$ mM min^{-1}), and K is the adsorption coefficient (20 mM^{-1}) of MB on the surface of TiO_2 particles. The latter is consistent with the low extent of MB adsorption on titania (see above).

MB degrades at relatively high initial concentrations (e.g., 0.3 mM) in UV-illuminated aqueous TiO_2 dispersions by first-order kinetics ($k_{app} = 1.5 \pm 0.1 \times 10^{-2}$ min^{-1}). Most of our experiments were run at an initial MB concen-

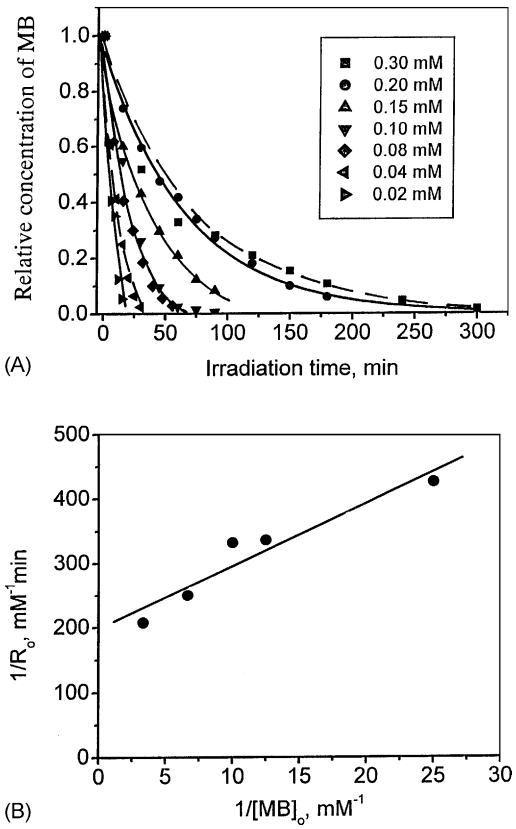

Fig. 8. Effect of initial concentration C_0 on the degradation of MB under UV irradiation (light irradiance, 3.6 mW/cm^2 at $\lambda = 360$ nm; pH 3.85; TiO_2 loading, 100 mg; MB/TiO_2 dispersion, 50 ml).

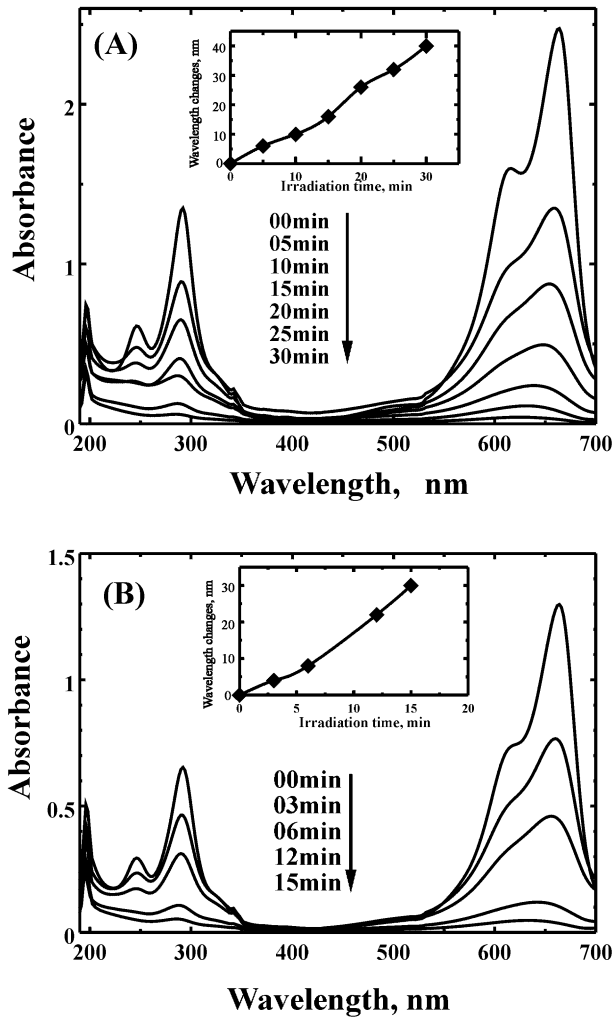

Fig. 9. Temporal spectral changes during the photodegradation of MB in dilute solutions. Initial concentrations are: (A) 0.04 mM and (B) 0.02 mM. Insets show the wavelength shifts (light irradiance, 3.6 mW/cm^2 at $\lambda = 360$ nm; pH 3.85; TiO_2 loading, 100 mg; MB/TiO_2 dispersion, 50 ml).

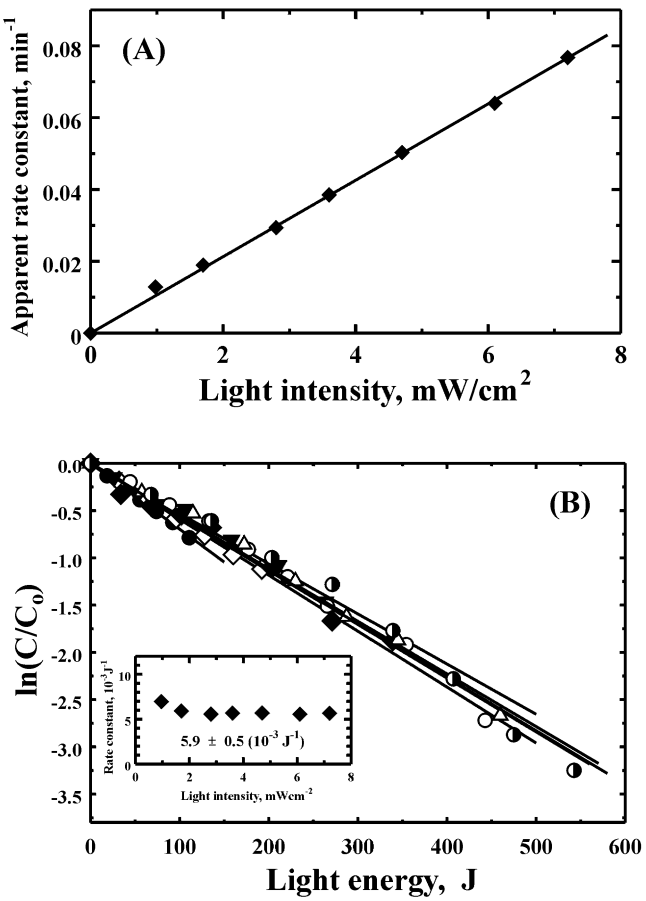

Fig. 10. (A) Plot showing the linear dependence of the apparent rate constants (min^{-1}) on light irradiance. (B) Plot showing the dependence of the concentration of MB undergoing degradation on the total light energy accumulated by TiO_2. Inset shows the light energy independence of the apparent rate constant (J^{-1}). Initial concentration of MB, 0.1 mM; pH 4.0; TiO_2 loading, 100 mg in a 50 ml dispersion. Light irradiance ($\lambda = 360$ nm): (●) 0.98 mW/cm^2, (◇) 1.7 mW/cm^2, (▼), 2.8 mW/cm^2, (◆) 3.6 mW/cm^2, (○) 4.7 mW/cm^2, (△) 6.1 mW/cm^2, and (◐) 7.2 mW/cm^2.

tration of 0.1 mM, at which the pertinent color changes of the TiO_2 particle surface were easily observed as a result of *N*-demethylation of MB. At lower concentrations of MB (e.g., 0.0066–0.036 mM [17]; 0.0267–0.112 mM [18]; 0.001–0.1 mM [15]) than otherwise used in the present study, the hypsochromic effect was not visually well defined because of slight color changes at the TiO_2 particle surface. Nonetheless, at MB concentrations of 0.02 or 0.04 mM, the hypsochromic effect could easily be observed by UV–visible spectral changes (Fig. 9).

3.6. Dependence of the photoreaction rate on light irradiance

Fig. 10A shows the linear dependence of the apparent rate constants (min^{-1}) on light irradiance (Eq. (3)),

$$k_{app} = 0.01065I \quad (3)$$

(Table 3; correlation coefficient, $r = 0.999$; I in mW/cm^2 at $\lambda = 360$ nm); they scale linearly with light irradiance (or photon flux). Under these reaction conditions, photons entering the reaction solution produce the corresponding quantity of photogenerated holes (h^+) which ultimately lead to oxidative photodegradation.

Table 3
Photodegradation kinetics and their dependence on light irradiance

Light irradiance (mW/cm^2)	k_{app} (10^{-2} min^{-1})
0.0	0.0
0.98	1.3
1.7	1.9
2.8	2.9
3.6	3.9
4.7	5.0
6.1	6.4
7.2	7.7

We next examined how the rate of degradation of MB may be affected by the total energy absorbed by the TiO_2 photocatalyst determined using Eq. (4):

$$E = S \int I \, dt \tag{4}$$

where E is the total absorbed energy (J), S the area of the illuminated photoreactor (cm^2), I the light intensity (mW/cm^2), t denotes the irradiation time (min) and $\int I \, dt$ represents the accumulated UV photon flux density (J/cm^2) reaching the light-harvesting surface of the photoreactor. Results shown in Fig. 10B which follow Eq. (5)

$$\ln\left(\frac{C}{C_0}\right) = -k_{obs}E \tag{5}$$

indicate that the rate of degradation of MB, k_{obs}, is independent of the total accumulated energy absorbed by the photocatalyst, $k_{obs} = 5.9 \pm 0.5 \times 10^{-3}\ J^{-1}$ in the range of light irradiance 0.98–7.2 mW/cm^2.

3.7. Temperature dependence of the photodegradation kinetics

The temperature dependence of the (apparent) kinetics, k_{app}, for the TiO_2-assisted photooxidative decomposition of MB shown in Fig. 11 was examined at four different temperatures in the range 21–68°C; estimated activation energy, $E_a = 8.9$ kJ/mol (Fig. 11B). Similarly, E_a's were reported for phenol (10 kJ/mol) [31], iprobenfos (12.5 kJ/mol) [29] and oxalic acid (13 kJ/mol) [32], but smaller than activation energies reported for 2-propanol (31 kJ/mol) [33] in TiO_2 dispersions and 48 kJ/mol for the oxidation of phenol by Fenton's reagent.

3.8. Relative photonic efficiency

Quantum yield as defined in homogeneous photochemistry is not an easily accessible parameter in heterogeneous photocatalytic systems because too many factors are ill-defined. An earlier study suggested employing the protocol of relative photonic efficiencies, ξ_r, which have been shown to be independent of light irradiance, reactor geometry and TiO_2 concentration for a given TiO_2 sample, but do seem to depend on the initial concentration of substrate, temperature and, to a lesser degree, on pH [13]. Phenol was selected as a secondary actinometer. The efficiency ξ_r was 0.48 determined under identical experimental conditions (initial concentration of reactant, 0.1 mM (50 ml); TiO_2, 100 mg (P-25); pH 4.0; light intensity, 4.7 mW/cm^2) by a protocol reported by Serpone et al. [13]. MB degrades less efficiently than phenol. Possibly, the complex constituents in the MB structure provide a much less efficient path for photocatalytic oxidation.

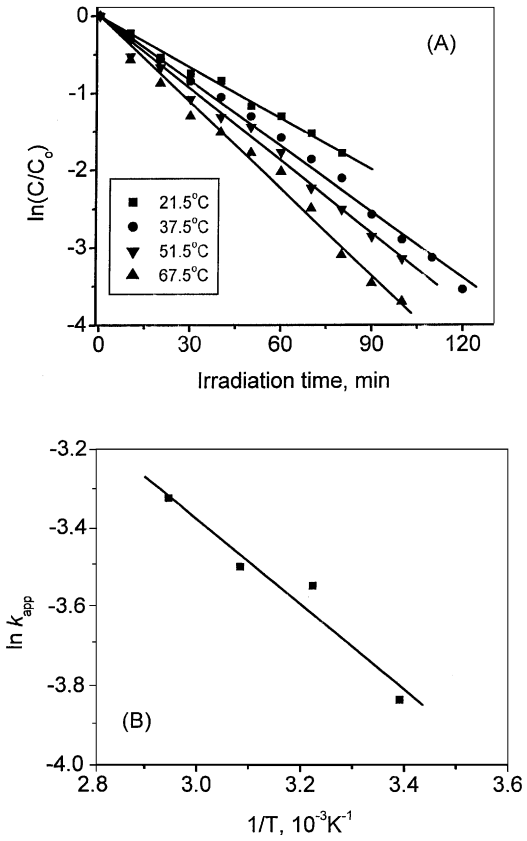

Fig. 11. Temperature dependence of the photocatalytic degradation of MB in 50 ml aqueous TiO_2 dispersions under UV light irradiation (MB, 0.1 mM; TiO_2 loading, 100 mg; pH 3.99; light irradiance, 7.0 mW/cm^2 at $\lambda = 360$ nm). (A) Kinetics of MB photodegradation in an aqueous TiO_2 dispersion at various temperatures (±1°C). (B) Arrhenius plot of the kinetics of photodegradation of MB taken from (A).

4. Concluding remarks

The photocatalyzed degradation of MB was examined by UV-illuminated aqueous TiO_2 dispersions, a representative of polluting dyestuffs in textile effluents. Hypsochromic effects resulting from *N*-demethylation of MB and oxidative degradation occurred concomitantly during irradiation. The degradative process was examined to assess the influence of several factors germane to possible scale-up of the technique to degrade pollutants. Photobleaching of MB occurs at low DOC owing to reduction of MB by photogenerated electrons not fully scavenged by the level of DOC in the dispersion. Color change from blue to colorless is reversible. The rate of degradation of MB was unaffected by the various methods used to introduce oxygen in the dispersions. As well, the kinetics of the photocatalytic process were independent of the total accumulated light energy absorbed by the TiO_2 particles, but increased proportionately with increase in light irradiance. The photoreaction occurred by good pseudo first-order kinetics even at high initial concentrations of MB (0.3 mM). Temperature had a relatively small effect on the MB degradation kinetics.

Acknowledgements

Our research in Tokyo was kindly supported by a Grants-in-aid for Science Research from the Ministry of Education of Japan (No. 10640569, to HH), in Beijing by the National Science Foundation of China (No. 29725715 and 29637010, to JZ), and in Montreal by the Natural Sciences and Engineering Research Council of Canada (to NS).

References

[1] R. Ganesh, G.D. Boardman, D. Michelson, Water Res. 28 (1994) 1367.
[2] E.J. Weber, R.L. Adams, Environ. Sci. Technol. 29 (1995) 113.
[3] R. Rossetti, L.E. Brus, J. Am. Chem. Soc. 106 (1984) 4336.
[4] K. Vinodgopal, P.V. Kamat, J. Photochem. Photobiol. A 83 (1994) 141.
[5] P.V. Kamat, S. Das, K.G. Thomas, M.V. George, Chem. Phys. Lett. 178 (1991) 75.
[6] J.J. He, J.C. Zhao, H. Hidaka, N. Serpone, J. Chem. Soc. Faraday Trans. 94 (1998) 2375.
[7] J.J. He, J.C. Zhao, T. Shen, H. Hidaka, N. Serpone, J. Phys. Chem. 101 (1997) 9027.
[8] P. Qu, J.C. Zhao, T. Shen, H. Hidaka, Colloids Surf. A 138 (1998) 39.
[9] P.V. Kamat, K. Vinodgopal, in: D.F. Ollis, H. Al-Ekabi (Eds.), Photocatalytic Purification and Treatment of Water and Air, Elsevier, Amsterdam, 1993, pp. 603–637.
[10] A.L. Linsebigler, G. Lu, J.T. Yates, Chem. Rev. 95 (1995) 735.
[11] K. Vinodgopal, D.E. Wynkoop, P.V. Kamat, Environ. Sci. Technol. 30 (1996) 1660.
[12] W.Z. Tang, H. Auren, Chemosphere 31 (1995) 4157.
[13] N. Serpone, G. Sauve, R. Koch, H. Tahiri, P. Pichat, P. Piccinini, E. Pelizzetti, H. Hidaka, J. Photochem. Photobiol. A 94 (1996) 191.
[14] D.F. Ollis, E. Pelizzetti, N. Serpone, in: N. Serpone, E. Pelizzetti (Eds.), Photocatalysis — Fundamentals and Applications, Wiley/Interscience, New York, 1989, pp. 603–637.
[15] R.W. Matthews, J. Chem. Soc. Faraday Trans. 1 85 (1989) 1291.
[16] P. Reeves, R. Ohlhausen, D. Sloan, K. Pamplin, T. Scoggins, Sol. Energy 48 (1992) 413.
[17] S. Lakshmi, R. Renganathan, S. Fujita, J. Photochem. Photobiol. A 88 (1995) 163.
[18] K. Sopajaree, S.A. Qasim, S. Basak, K. Rajeshwar, J. Appl. Electrochem. 29 (1999) 533.
[19] M. Windholz, The Merck Index, 10th Edition, Merck & Co., Rahway, 1983.
[20] M.R. Hoffmann, S.T. Martin, W. Choi, D.W. Bahnemann, Chem. Rev. 95 (1995) 69.
[21] P.V. Kamat, Chem. Rev. 93 (1993) 267.
[22] P. Qu, J.C. Zhao, T. Shen, H. Hidaka, J. Mol. Catal. A 129 (1998) 257.
[23] T.X. Wu, G.M. Liu, J.C. Zhao, H. Hidaka, N. Serpone, J. Phys. Chem. B 102 (1998) 5845.
[24] T. Watanabe, T. Takizawa, K. Honda, J. Phys. Chem. 81 (1977) 1845.
[25] T. Takizawa, T. Watanabe, K. Honda, J. Phys. Chem. 82 (1978) 1391.
[26] T. Inoue, T. Watanabe, A. Fujishima, K. Honda, K. Kobayakawa, J. Electrochem. Soc. 124 (1977) 719.
[27] T. Mohammad, H. Morrison, J. Photochem. Photobiol. 71 (2000) 369.
[28] J.C. Zhao, H. Hidaka, A. Takamura, E. Pelizzetti, N. Serpone, Langmuir 9 (1989) 1646.
[29] K. Hasegawa, T. Kanbara, S. Kagaya, Denki Kagaku 66 (1998) 625.
[30] Editorial Committee, Encyclopaedia Chim. 9 (1960) 211A.
[31] K. Okamoto, Y. Yamamoto, H. Tanaka, A. Itaya, Bull. Chem. Soc. Jpn. 58 (1985) 2023.
[32] J.-M. Herrmann, M.N. Mozzanega, P. Pichat, J. Photochem. 22 (1983) 333.
[33] P.R. Harry, R. Rudham, S. Ward, J. Chem. Soc. Faraday Trans. 1 79 (1983) 291.